

Synthesis of Stable Shape-Controlled Catalytically Active β -Palladium Hydride

Zipeng Zhao,[†] Xiaoqing Huang,[†] Mufan Li,[§] Gongming Wang,[§] Chain Lee,[§] Enbo Zhu,[†] Xiangfeng Duan,^{§,‡} and Yu Huang^{*,†,‡}

[†]Department of Materials Science and Engineering, [§]Department of Chemistry and Biochemistry, and [‡]California Nanosystems Institute, University of California, Los Angeles, California 90095, United States

S Supporting Information

ABSTRACT: We have developed an efficient strategy for the production of stable β -palladium hydride ($\text{PdH}_{0.43}$) nanocrystals with controllable shapes and remarkable stability. The as-synthesized $\text{PdH}_{0.43}$ nanocrystals showed impressive stability in air at room temperature for over 10 months, which has enabled the investigation of their catalytic property for the first time. The prepared $\text{PdH}_{0.43}$ nanocrystals served as highly efficient catalysts in the oxidation of methanol, showing higher activity than their Pd counterparts. These studies opened a door for further exploration of β -palladium hydride-based nanomaterials as a new class of promising catalytic materials and beyond.

Palladium-hydrogen system, including palladium hydride material, is a long known system that attracts broad interest for their potential applications as hydrogen sensor,^{1–3} hydrogen storage,^{4,5} and hydrogen purification.^{6,7} Particularly, the β -phase palladium hydride garnered considerable attention due to its high hydrogen capacity.^{8,9} The preparations of β -palladium hydride nanostructures have been demonstrated by directly exposing surface cleaned palladium nanomaterials to hydrogen gas,¹⁰ applying negative potential to palladium in electrochemical cell,¹¹ and by heating palladium nanostructures in NaBH_4 solution.^{12,13} A recent work reported the synthesis of shaped palladium hydride nanocrystals.¹⁴ However, studies on the shape-controlled synthesis of β -palladium hydride nanostructures have been sparse, and the reported palladium hydride nanostructures were not stable, preventing further studies of this interesting nanomaterial system.

Here we report efficient strategies enabling the synthesis of stable, shape-controlled β -palladium hydride nanocrystals and show that these are promising catalysts for chemical reactions. In a typical one-step synthesis, 8 mg palladium(II) acetylacetonate ($\text{Pd}(\text{acac})_2$) was mixed with 10 mL N,N -dimethylformamide (DMF). The solution was then kept at 160 °C for 4h before it was cooled down to room temperature. The products were collected by centrifuge and washed several times with ethanol for following characterizations (Figure 1). Selected area electron diffraction (SAED) pattern (Figure 1A) of the resulting material (Figure 1B top inset) indicated a polycrystal sample of fcc structure with a lattice parameter of around 0.400 nm, 2.8% larger than that of the palladium (0.389 nm). At the same time, energy dispersive spectrum (EDS) test showed only palladium present (Figure S1A) ruling out the

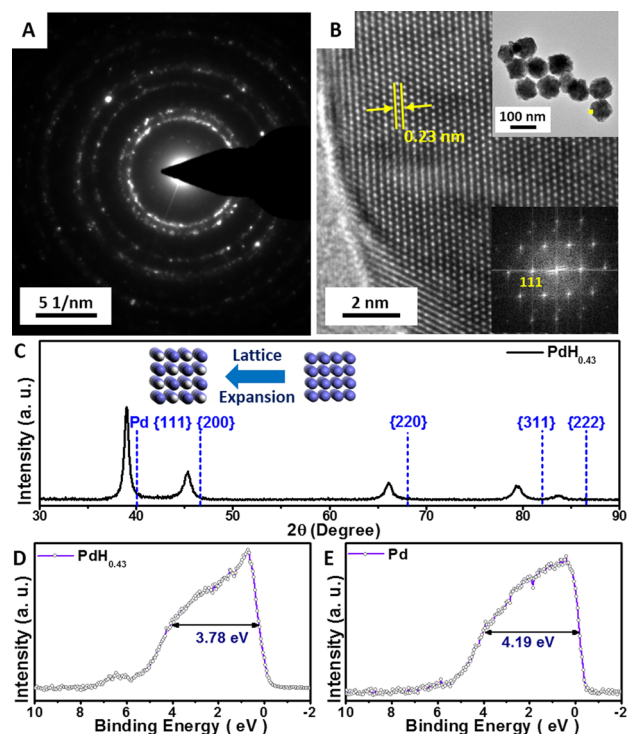


Figure 1. (A) SAED of $\text{PdH}_{0.43}$ nanocrystals. (B) HRTEM image of $\text{PdH}_{0.43}$, top inset: TEM image of the $\text{PdH}_{0.43}$ nanocrystals where SAED was taken, yellow dot indicated the area where HRTEM was taken; bottom inset: FFT of HRTEM. (C) XRD of β -palladium hydride. XPS valence band structure of (D) $\text{PdH}_{0.43}$ and (E) Pd.

existence of impurities. High-resolution transmission electron microscopy (HRTEM) image (Figure 1B) of the resulting crystal, together with fast Fourier transform (FFT) (Figure 1B bottom inset), showed a $\{111\}$ interplane distance of 0.231 nm, again consistent with fcc structure with a lattice parameter around 0.400 nm.

The powder X-ray diffraction (XRD) (Figure 1C) pattern indicated fcc packing with a lattice parameter around 0.3996 nm, consistent with transmission electron microscopy (TEM) observation. The XRD pattern also suggests the resulting material to be β -palladium hydride, with an H:Pd ratio of 0.43

Received: November 4, 2015

Published: December 4, 2015

based on lattice parameter and composition relationship within palladium-hydrogen system.^{15–18} In order to further confirm the formation of PdH_{0.43}, we used X-ray photoelectron spectroscopy (XPS) to extract valence band structures (Figure 1D,E) of Pd and PdH_{0.43}, which showed bandwidth of 4.19 eV for Pd and 3.78 eV for PdH_{0.43}, respectively. Additionally on the band structure of PdH_{0.43}, a peak close to the Fermi level at 0.71 eV and a small shake up close to the end of the valence band at 6.39 eV were also observed, consistent with reported values for β -palladium hydride.^{19–24} Furthermore, the Pd 3d core of PdH_{0.43} shifted 0.29 eV to higher binding energy compared to that of Pd (Figure S1B), also consistent with previous report.²²

Importantly, our PdH_{0.43} nanocrystals showed much higher stability compared to previous reports.^{10–14} After 10 months' storage in air at room temperature, no change was observed in XRD spectra, indicating stable structures and composition (Figure S2A). Even in the annealing test at elevated temperatures, PdH_{0.43} nanocrystals showed no significant XRD change after 2 h annealing at 300 °C in Ar (Figure S2B). Interestingly when H₂ is introduced into the annealing atmosphere, transformation from PdH_{0.43} to Pd was observed (Figure S2C). We suggest the original PdH_{0.43} surface might have been passivated with minute oxide, leading to the excellent stability and that extra H₂ in the annealing atmosphere may activate Pd surface for hydrogen release, although the exact mechanism for the remarkable PdH_{0.43} stability demands further studies.

To understand the formation process of PdH_{0.43} nanocrystals during synthesis, we tracked the products at different durations into the reaction. It was observed that the solution color turned from orange to black at 15 min into the reaction. XRD of the product collected at this point indicated the formation of pure palladium. Around 30 min into the reaction, XRD spectrum indicates a lattice parameter of 0.3970 nm, corresponding to H:Pd ratio around 0.33. And after 1 h, XRD peak shifted to even a lower angle, showed a lattice parameter of 0.3993 nm, and corresponded H:Pd ratio around 0.42. No significant shift of XRD peaks was observed at 4 h compared to 1 h, with a lattice parameter of 0.3996 nm (Figure 2A, Table S1) and H:Pd ratio around 0.43. The XPS valence band spectra also showed the same change from Pd to PdH_{0.43} (Figure 2B). These observations suggest that Pd nanocrystals formed first and then

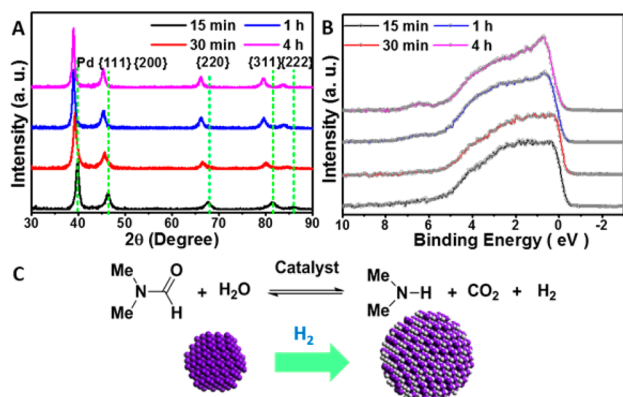


Figure 2. Time tracking (A) XRD during the synthesis of PdH_{0.43} with reaction times of 15 min, 30 min, 1 h and 4 h and (B) XPS during the synthesis of PdH_{0.43} with reaction times 15 min, 30 min, 1 h and 4 h. (C) Schematic about formation of PdH_{0.43} in DMF.

transformed *in situ* to PdH_{0.43}. As it was reported that catalytic decomposition of DMF can produce hydrogen gas *in situ*,^{25–27} we suggest that the catalytic decomposition of DMF on the surface of the initially formed Pd nanocrystals provided hydrogen gas, which then was absorbed into the Pd nanocrystals to form PdH_{0.43} at the later growth stage. Indeed, the production of hydrogen gas during reaction was detected with gas chromatography coupled with barrier discharge ionization detector, which provided direct evidence that the decomposition of DMF provided hydrogen source for the formation of PdH_{0.43} during synthesis (Figure S5). In addition, our control experiments without DMF, but with ethylene glycol and benzyl alcohol, while keeping other conditions same, showed no β -palladium hydride formation (Figure S4A), indicating the key role of DMF during the synthesis of PdH_{0.43}. In another control, when Pd(acac)₂ was replaced with Na₂PdCl₄, the β -palladium hydride phase could still form in the presence of DMF (Figure S4B), suggesting precursors did not play import roles in PdH_{0.43} formation.

Understanding the formation process of PdH_{0.43}, particularly the role of DMF in providing hydrogen *in situ* to transform the preformed Pd nanocrystals, we further showed that we could transform presynthesized pure Pd nanocrystals into β -palladium hydride phase by annealing them in DMF at 160 °C for 16h (Figure S4C). Following this success, we designed a two-step approach to achieve shape-controlled synthesis of β -palladium hydride nanostructures using presynthesized Pd nanocrystals. Pd nano-polycrystals (Figure 3A), nano-tetrahedra (Figure 3B), and nanocubes (Figure 3C) were synthesized using reported methods,²⁸ which were then dispersed and annealed in DMF at 160 °C for 16 h. The transformation from Pd to β -palladium hydride was achieved for all Pd nanostructures treated, and it

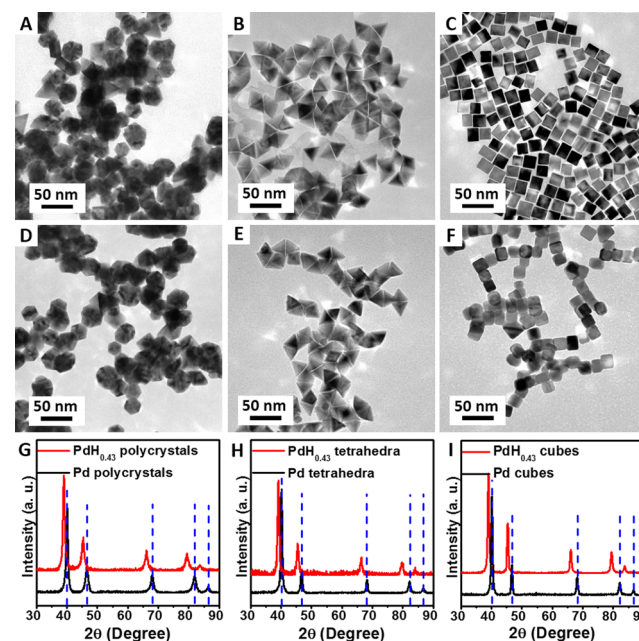


Figure 3. TEM images of (A) Pd nano-polycrystals, (B) Pd nano-tetrahedra, (C) Pd nanocubes, (D) PdH_{0.43} nano-polycrystals, (E) PdH_{0.43} nano-tetrahedra, and (F) PdH_{0.43} nanocubes. (G) XRD comparison of Pd nano-polycrystal before (A) and after conversion (D). (H) XRD comparison of Pd nano-tetrahedra before (B) and after conversion (E). (I) XRD comparison of Pd nanocubes before (C) and after conversion (F).

was found that their shapes were maintained after the transformation (Figure 3D–F). All final β -palladium hydride nanocrystals were confirmed by XRD (Figure 3G–I) to be $\text{PdH}_{0.43}$. HRTEM, FFT (Figure S6), and XPS valence band structure (Figure S7) showed consistent results, confirming successful conversion from Pd to $\text{PdH}_{0.43}$.^{18–23} Additionally, stability studies showed these $\text{PdH}_{0.43}$ nanostructures (nano-polycrystals, nano-tetrahedra, nanocubes) similar stability (Figure S8).

After successfully obtaining stable and well-shaped Pd and $\text{PdH}_{0.43}$ nanostructures, we explored the catalytic properties of these $\text{PdH}_{0.43}$ nanocrystals and compared them to their pure Pd counterparts (Table 1, Figure 4).

Table 1. Comparison of Catalytic Activities of Pd and $\text{PdH}_{0.43}$ in Methanol Oxidation Reaction with Specific Activity Compared at 0.85 V vs Reverse Hydrogen Electrode

| samples | specific activity (mA/cm^2) |
|---|---|
| Pd nano-polycrystals | 0.822 |
| $\text{PdH}_{0.43}$ nano-polycrystals | 1.046 |
| Pd nano-tetrahedra on carbon | 0.886 |
| $\text{PdH}_{0.43}$ nano-tetrahedra on carbon | 1.228 |

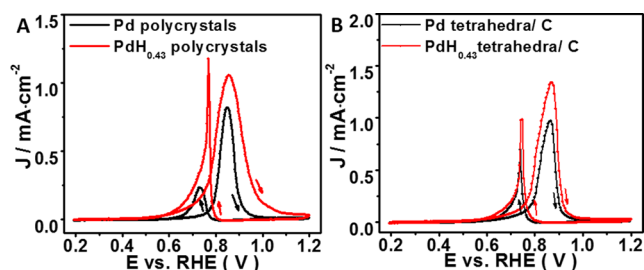


Figure 4. CV of methanol oxidation, performed in N_2 saturated, 0.1 M KOH with 0.1 M methanol, scan rate is 10 mV/s, normalized by electrochemical surface area. Comparison between (A) Pd nano-polycrystals and $\text{PdH}_{0.43}$ nano-polycrystals and (B) Pd nano-tetrahedra and $\text{PdH}_{0.43}$ nano-tetrahedra.

We chose electrochemical methanol oxidation reaction (MOR) in alkaline media as a model reaction to test the catalytic properties of these $\text{PdH}_{0.43}$ nanocrystals. In addition their activities were compared to those of the Pd nanostructure counterparts before the transformation (Figures 3A,D,G and S9). It was found that $\text{PdH}_{0.43}$ showed higher MOR specific activity compared to Pd (Table 1) for both nano-polycrystals and nano-tetrahedra. In addition, we observed that during CO stripping test (Figure S10), the CO stripping peak showed up at lower voltage on $\text{PdH}_{0.43}$ compared to Pd, indicating weaker CO adsorption on $\text{PdH}_{0.43}$, possibly resulting from the larger lattice parameter and the different valence band structure of $\text{PdH}_{0.43}$. As CO is a known intermediate during MOR, whose presence can poison the catalysts,^{29,30} we suggest that the weaker CO binding on $\text{PdH}_{0.43}$ helps to enhance its catalytic efficiency in MOR. In addition it was observed that $\text{PdH}_{0.43}$ tetrahedra showed better activity than $\text{PdH}_{0.43}$ polycrystals, showing a similar trend as Pd nanocrystals with {111} facet showed better electrochemistry activity than Pd black, which is polycrystalline.¹⁴

In summary, we have developed a simple yet efficient approach to obtain stable β - $\text{PdH}_{0.43}$ with controllable shapes, utilizing the *in situ* produced hydrogen gas from the catalytic decomposition of DMF to transform Pd nanocrystals in

solution. Importantly the obtained $\text{PdH}_{0.43}$ nanostructures showed remarkably high stability for palladium hydrides, remaining stable for 2 h under 300 °C in Ar and up to 10 months at room temperature in air. The ability to obtain stable and shaped $\text{PdH}_{0.43}$ allowed us to explore the catalytic properties of $\text{PdH}_{0.43}$ for the first time. It was found that $\text{PdH}_{0.43}$ is indeed catalytically active and showed higher catalytic activity for MOR when compared to the Pd counterparts. It was also revealed that faceted $\text{PdH}_{0.43}$ nanocrystals showed better activity than its polycrystal counterparts, which is worthy of further exploration for property tailoring. The remarkable stability demonstrated in palladium hydride nanostructures can open up great opportunities for exploring this material system for various applications.

■ ASSOCIATED CONTENT

📄 Supporting Information

The Supporting Information is available free of charge on the ACS Publications website at DOI: 10.1021/jacs.5b11543.

Detailed synthesis, characterization results, and additional electrochemical data (PDF)

■ AUTHOR INFORMATION

Corresponding Author

*yhuang@seas.ucla.edu

Notes

The authors declare no competing financial interest.

■ ACKNOWLEDGMENTS

We acknowledge the support from National Science Foundation (NSF) through award no. DMR-1437263. X.D. acknowledges the support from the U.S. Department of Energy, Office of Basic Energy Sciences, Division of Materials Science and Engineering through Award DE-SC0008055. We also thank Electron Imaging Center of Nanomachines at CNSI for the TEM support.

■ REFERENCES

- (1) Favier, F.; Walter, E. C.; Zach, M. P.; Benter, T.; Penner, R. M. *Science* **2001**, *293*, 2227.
- (2) Yang, F.; Kung, S.-C.; Cheng, M.; Hemminger, J. C.; Penner, R. M. *ACS Nano* **2010**, *4*, 5233.
- (3) Zeng, X. Q.; Latimer, M. L.; Xiao, Z. L.; Panuganti, S.; Welp, U.; Kwok, W. K.; Xu, T. *Nano Lett.* **2011**, *11*, 262.
- (4) Horinouchi, S.; Yamanoi, Y.; Yonezawa, T.; Mouri, T.; Nishihara, H. *Langmuir* **2006**, *22*, 1880.
- (5) Li, G.; Kobayashi, H.; Taylor, J. M.; Ikeda, R.; Kubota, Y.; Kato, K.; Takata, M.; Yamamoto, T.; Toh, S.; Matsumura, S.; Kitagawa, H. *Nat. Mater.* **2014**, *13*, 802.
- (6) Uemiyama, S.; Sato, N.; Ando, H.; Kude, Y.; Matsuda, T.; Kikuchi, E. *J. Membr. Sci.* **1991**, *56*, 303.
- (7) Adhikari, S.; Fernando, S. *Ind. Eng. Chem. Res.* **2006**, *45*, 875.
- (8) Flanagan, T. B.; Oates, W. A. *Annu. Rev. Mater. Sci.* **1991**, *21*, 269.
- (9) Manchester, F. D.; San-Martin, A.; Pitre, J. M. *J. Phase Equilib.* **1994**, *15*, 62.
- (10) Bardhan, R.; Hedges, L. O.; Pint, C. L.; Javey, A.; Whitlam, S.; Urban, J. J. *Nat. Mater.* **2013**, *12*, 905.
- (11) Rose, A.; Maniguet, S.; Mathew, R. J.; Slater, C.; Yao, J.; Russell, A. E. *Phys. Chem. Chem. Phys.* **2003**, *5*, 3220.
- (12) Murphy, D. W.; Zahurak, S. M.; Vyas, B.; Thomas, M.; Badding, M. E.; Fang, W. C. *Chem. Mater.* **1993**, *5*, 767.
- (13) Phan, T.-H.; Schaak, R. E. *Chem. Commun.* **2009**, 3026.
- (14) Dai, Y.; Mu, X.; Tan, Y.; Lin, K.; Yang, Z.; Zheng, N.; Fu, G. J. *Am. Chem. Soc.* **2012**, *134*, 7073.

- (15) Schirber, J. E.; Morosin, B. *Phys. Rev. B* **1975**, *12*, 117.
- (16) Worsham, J. E., Jr; Wilkinson, M. K.; Shull, C. G. *J. Phys. Chem. Solids* **1957**, *3*, 303.
- (17) Eastman, J. A.; Thompson, L. J.; Kestel, B. J. *Phys. Rev. B: Condens. Matter Mater. Phys.* **1993**, *48*, 84.
- (18) Wolf, R. J.; Lee, M. W.; Ray, J. R. *Phys. Rev. Lett.* **1994**, *73*, 557.
- (19) Eastman, D. E.; Cashion, J. K.; Switendick, A. C. *Phys. Rev. Lett.* **1971**, *27*, 35.
- (20) Wagner, F. E.; Wortmann, G. *Hydrogen in Metals I*; Alefeld, G., Völkl, J., Eds.; Springer: Berlin Heidelberg, 1978; pp 28, 131.
- (21) Bennett, P. A.; Fuggle, J. C. *Phys. Rev. B: Condens. Matter Mater. Phys.* **1982**, *26*, 6030.
- (22) Riesterer, T. *Z. Phys. B: Condens. Matter* **1987**, *66*, 441.
- (23) Hofmann, T.; Yu, T. H.; Folse, M.; Weinhardt, L.; Bär, M.; Zhang, Y.; Merinov, B. V.; Myers, D. J.; Goddard, W. A.; Heske, C. *J. Phys. Chem. C* **2012**, *116*, 24016.
- (24) Eberhardt, W.; Louie, S. G.; Plummer, E. W. *Phys. Rev. B: Condens. Matter Mater. Phys.* **1983**, *28*, 465.
- (25) Yu, J. Y.; Schreiner, S.; Vaska, L. *Inorg. Chim. Acta* **1990**, *170*, 145.
- (26) Wan, Y.; Alterman, M.; Larhed, M.; Hallberg, A. *J. Org. Chem.* **2002**, *67*, 6232.
- (27) Heim, L. E.; Schlörer, N. E.; Choi, J.-H.; Precht, M. H. G. *Nat. Commun.* **2014**, *5*, 3621.
- (28) Jin, M.; Liu, H.; Zhang, H.; Xie, Z.; Liu, J.; Xia, Y. *Nano Res.* **2011**, *4*, 83.
- (29) Wasmus, S.; Küver, A. *J. Electroanal. Chem.* **1999**, *461*, 14.
- (30) Liu, H.; Song, C.; Zhang, L.; Zhang, J.; Wang, H.; Wilkinson, D. *P. J. Power Sources* **2006**, *155*, 95.